Induction of G_1 Arrest by SB265610 Involves Cyclin D3 Down-regulation and Suppression of CDK2 (Thr160) Phosphorylation

AHMED E. GODA[1,3], RAYMOND L. ERIKSON[1,2], JONG-SEOG AHN[4] and BO-YEON KIM[1]

[1]*World Class Institute, Incurable Diseases Therapeutics Research Center, and* [4]*Chemical Biology Research Center, Korea Research Institute of Bioscience and Biotechnology, Ochang, Cheongwon, Republic of Korea;*
[2]*Department of Molecular and Cellular Biology, Harvard University, Cambridge, MA, U.S.A.;*
[3]*Department of Pharmacology and Toxicology, Faculty of Pharmacy, Tanta University, Tanta, Egypt*

Abstract. *Background/Aim: The current study investigated the mechanisms underlying the antitumor activity of SB265610, a cysteine-amino acid-cysteine (CXC) chemokines receptor 2 (CXCR2) antagonist. Materials and Methods: Cell-cycle progression and regulatory molecules were assessed by flow cytometry, immunoblotting, real-time PCR and immunoprecipitation. Target validation was achieved via RNA interference. Results: G_1 arrest induced by SB265610 occurred at concentrations lacking CXCR2 selectivity, persisted upon interleukin 8 (IL8) challenge, and did not affect IL8 downstream target expression. Profiling of G_1 regulators revealed cyclin-dependent kinase 2 (CDK2) (Thr160) hypophosphorylation, cyclin D3 gene down-regulation, and p21 post-translational induction. However, only cyclin D3 and CDK2 contributed towards G_1 arrest. Furthermore, SB265610 induced a sustained phosphorylation of the p38MAPK. Pharmacological interference with p38MAPK significantly abrogated SB265610-induced G_1 arrest and normalized the expression of cyclin D3, with restoration of its exclusive binding to CDK6, but with weak recovery of CDK2 (Thr160) hypo-phosphorylation. Conclusion: The present study described the mechanisms for the anti-proliferative activity of SB265610 which may be of value in IL8-rich tumor microenvironments.*

Human cancers of different origins, including breast, gastric, colon, melanoma, ovarian, pancreatic and prostatic, have been shown to express elevated levels of the pro-inflammatory chemokine interleukin-8 (IL8, CXCL8) compared to the surrounding normal tissues. Cancer cells can further increase IL8 synthesis and secretion following chemotherapy or as a result of hypoxia (1). Two G-protein-coupled receptors namely, cysteine-amino acid-cysteine (CXC) chemokine receptor 1 (CXCR1) and CXCR2 are expressed on cancer cells, as well as tumor-associated vascular endothelial cells and macrophages, and differentially mediate the complex autocrine/paracrine signaling of IL8 and other Glu-Leu-Arg tripeptide motif (ELR^+) CXC chemokines within the tumor micro-environment where both CXCR1 and CXCR2 receptors are activated by IL8 and granulocyte chemotactic peptide-2 (CXCL6). However, only CXCR2 receptors are activated by several other ELR^+ CXC chemokines, such as those with melanoma growth-stimulatory activities (CXCL1, CXCL2, CXCL3), epithelial neutrophil-activating protein (CXCL5) and neutrophil-activating protein (CXCL7) (1, 2). Elevated levels of IL8 and other ELR^+ CXC chemokines have been shown to drive the proliferation, angiogenesis and migration of cancer cells and tumor-associated vascular endothelial cells, with a relatively higher contribution of CXCR2 receptors to these processes (1, 3).

Over the past two decades several small-molecule receptor antagonists belonging to different chemical classes have been developed to target IL8 receptors in a competitive or allosteric manner and with varying degrees of selectivity towards CXCR1 or CXCR2 receptors or acting as dual CXCR1/2 inhibitors (2). In our previous work we identified novel off-target antitumor mechanisms for the compound SB225002, a highly selective CXCR2 antagonist of the diarylurea nucleus, which enable this compound to dually-target cancer through microtubule destabilization and inhibition of IL8-driven cancer progression (4). In the current study, we investigated whether SB265610, a highly selective CXCR2 antagonist and a close structural analog of SB225002, may exert antitumor activity through IL8-independent mechanism(s).

Correspondence to: Bo-Yeon Kim, Ph.D., World Class Institute, Incurable Diseases Therapeutics Research Center, Korea Research Institute of Bioscience and Biotechnology, 685-2 Ochang, Cheongwon 363-883, Republic of Korea. Tel: +82 432406100, Fax: +82 432406259, e-mail: bykim@kribb.re.kr

Key Words: SB265610, G_1 arrest, cyclin D3, phospho(Thr160)-CDK2, p21, p38MAPK.

Materials and Methods

Chemicals. SB265610 (Tocris, Bristol, UK) was dissolved in dimethyl sulfoxide (DMSO), aliquoted and stored at −80˚C for no more than one week. Recombinant human IL8 (Biolegend, San Diego, CA, USA) was prepared in sterile phosphate buffered saline (PBS) containing 0.5% bovine serum albumin, aliquoted and stored at −80˚C. Two specific chemical inhibitors of p38 mitogen-activated protein kinase (p38MAPK), namely SB202190 and SB203580 (Tocris), were dissolved in DMSO, aliquoted and stored at −80˚C. Freeze-thaw cycles were avoided for all chemicals.

Cell culture. PC-3 androgen-independent human prostate adenocarcinoma cell line (American Type Culture Collection, Manassas, VA, USA) was cultured in RPMI 1640 medium (Hyclone, Logan, Utah, USA) supplemented with 10% fetal bovine serum (Hyclone, Logan, Utah, USA), L-glutamine (2 mmol/l), penicillin (100 units/ml), and streptomycin (100 μg/ml) (Gibco, Life Technologies, Grand Island, NY, USA) and maintained at 37˚C in a humidified atmosphere of 5% CO_2. Cell cultures at 50% confluence level were treated with SB265610, IL8 or p38MAPK chemical inhibitors as detailed in legends to figures.

Analysis of the cell cycle by flow cytometry. At the end of drug treatments, cells were harvested for cell-cycle analysis as described previously (5), where PC-3 cells were washed once with PBS, trypsinized and harvested. After washing twice with PBS at 500xg and 4˚C, cells were resuspended in PBS containing RNAse (100 μg/ml) Triton-X-100 (1 μl/ml) and propidium iodide (2.5 μg/ml) (all Sigma-Aldrich, St. Louis, MO, USA) and were analyzed (after 30 min and protected from light) on a BD FACSCalibur flow cytometer using CellQuest software package (BD Biosciences, San Jose, CA, USA). Data representative of three independent experiments (triplicates in each) are presented as the mean±SEM. Differences were considered statistically significant at $p<0.05$ using the Student's *t*-test.

Immunoblotting. Protein isolation and immunoblotting were performed as previously described (5). At the end of drug treatments, PC-3 cells were washed with ice-cold PBS and harvested using Pierce lysis buffer supplemented with protease and phosphatase inhibitor cocktails (Pierce, Rockford, IL, USA). Protein assay was performed on cell lysates using protein dye concentrate (BioRad, Hercules, CA, USA) and 40 μg of each sample were boiled in sodium dodecyl sulfate sample buffer (BioRad) before being resolved onto sodium dodecyl sulfate-polyacrylamide gel electrophoresis (SDS-PAGE). After blotting, polyvinylidene fluoride membranes (Pierce) were blocked for 1 h in 5% non-fat dry milk (Bio-Rad) in TBS-T and were incubated at room temperature for 2 h with the following primary antibodies: rabbit antihuman-cyclin D1, rabbit antihuman- retinoblastoma (RB), rabbit antihuman-cyclin-dependent kinase 2 (CDK2), mouse antihuman-CDK4, rabbit antihuman-CDK6, rabbit antihuman-cyclin E (Santa Cruz Biotechnology, Dallas, TX, USA); mouse antihuman-phospho extracellular signal-regulated kinase (ERK), rabbit antihuman-ERK, rabbit antihuman-phospho IKKα/β, rabbit antihuman-phospho RB (Ser795), rabbit antihuman-cyclin D2, mouse antihuman-cyclin D3, mouse antihuman-p21, rabbit antihuman-p27, rabbit antihuman-phospho CDK2 (Thr160), rabbit antihuman-p38MAPK, rabbit antihuman-phospho p38MAPK (Cell Signaling Technologies, Danvers, MA, USA); mouse antihuman-β-actin (Sigma-Aldrich). After washing in 5% non-fat dry milk (BioRad) in TBS-T, membranes were probed for 1 hour at room temperature with the appropriate secondary antibodies: horseradish peroxidase (HRP)-conjugated anti-rabbit IgG, HRP-conjugated anti-mouse IgG (Cell Signaling Technologies). The resulting chemiluminescence (Pierce) was recorded on X-ray films (Agfa, Mortsel, Belgium).

Immunoprecipitation (IP). All IP steps were carried out on ice. PC-3 cells were harvested in IP lysis buffer (Pierce) supplemented with protease and phosphatase inhibitor cocktails (Pierce) and were disrupted by repeated aspiration through a 21-gauge needle. Cell lysates were recovered by centrifugation at 21000xg at 4˚C. Five hundred micrograms of protein of the cell lysates were immunoprecipitated by incubation with 2 μg of antibodies for CDK4, CDK6 or IgG control antibody in a total volume of 750 μl with rotation at 4˚C overnight followed by incubation with 40 μl of protein A/G-agarose beads (Santa Cruz Biotechnology) for 4 h at 4˚C. Immunoprecipitates were collected by centrifugation at 600 xg for 5 min at 4˚C. After washing five times with IP lysis buffer, immunoprecipitates were resuspended and boiled in 40 μl SDS sample buffer and resolved by SDS-PAGE. Co-immunoprecipitated cyclin D3 was detected by immunoblotting.

siRNA-mediated knockdown of gene expression. To knockdown *CDKN1A* (p21) expression, two commercially available and validated siRNA sequences #1029367 and #1029372 were purchased from Bioneer Corporation (Daejeon, Republic of Korea). In addition, a third previously described *CDKN1A* (p21) siRNA sequence (6) was synthesized by Bioneer Corporation. These three different *CDKN1A* (p21)-targeting sequences are referred to herein as sip21#1, sip21#2 and sip21#3, respectively. For the knockdown of *CCND3* (cyclin D3) and *CDK2*, commercially available and validated *CCND3* (cyclin D3) siRNA sequence (#1027310) and *CDK2* siRNA sequence (#1029167), as well as the non-targeting *LacZ* siRNA control sequence (7) were ordered from Bioneer Corporation. All siRNA sequences were transfected (at 100 nM final concentration) into PC-3 cells using Lipofectamine™ RNAiMAX Transfection Reagent (Invitrogen, Life Technologies, Grand Island, NY, USA) according to the manufacturer's instructions. Knockdown efficiency was assessed by immunoblotting. Data representative of three independent experiments (triplicates in each) are presented as the mean±SEM. Differences were considered statistically significant at $p<0.05$ using Student's *t*-test.

RNA extraction and real-time PCR. At the end of drug treatments, PC-3 cells were harvested in Trizol reagent (Life Technologies) according to the manufacturer's instructions. RNA was recovered from the aqueous layer using RNeasy Mini Kit (Qiagen, Hilden, Germany) as recommended by the manufacturer. First-stand cDNA was synthesized using AccuPower® CycleScript RT PreMix (dT20) (Bioneer Corporation) according to the manufacturer's instructions. For real-time PCR analysis, the following primer pairs were used at 350 nM final concentration: p21 sense: 5`-CGATGCCAACCTCCTCAACGA-3`, p21 antisense: 5`-TCGCAGACCTCCAGCATCCA-3` (8); cyclin D3 sense: 5`-TGGATGCTGGAGGTATGTG-3`, cyclin D3 antisense: 5`-CGTGGTCGGTGTAGATGC-3`(9). SYBR® Green Real-Time PCR Master Mix (Toyobo, Osaka, Japan) was used with the following manufacturer recommended cycling conditions: 95˚C for 60 sec followed by 50 cycles of 95˚C for 15 sec, 60˚C for 15 sec, and 72˚C for 60 sec. The final PCR reaction volume/well was 25 μl (containing

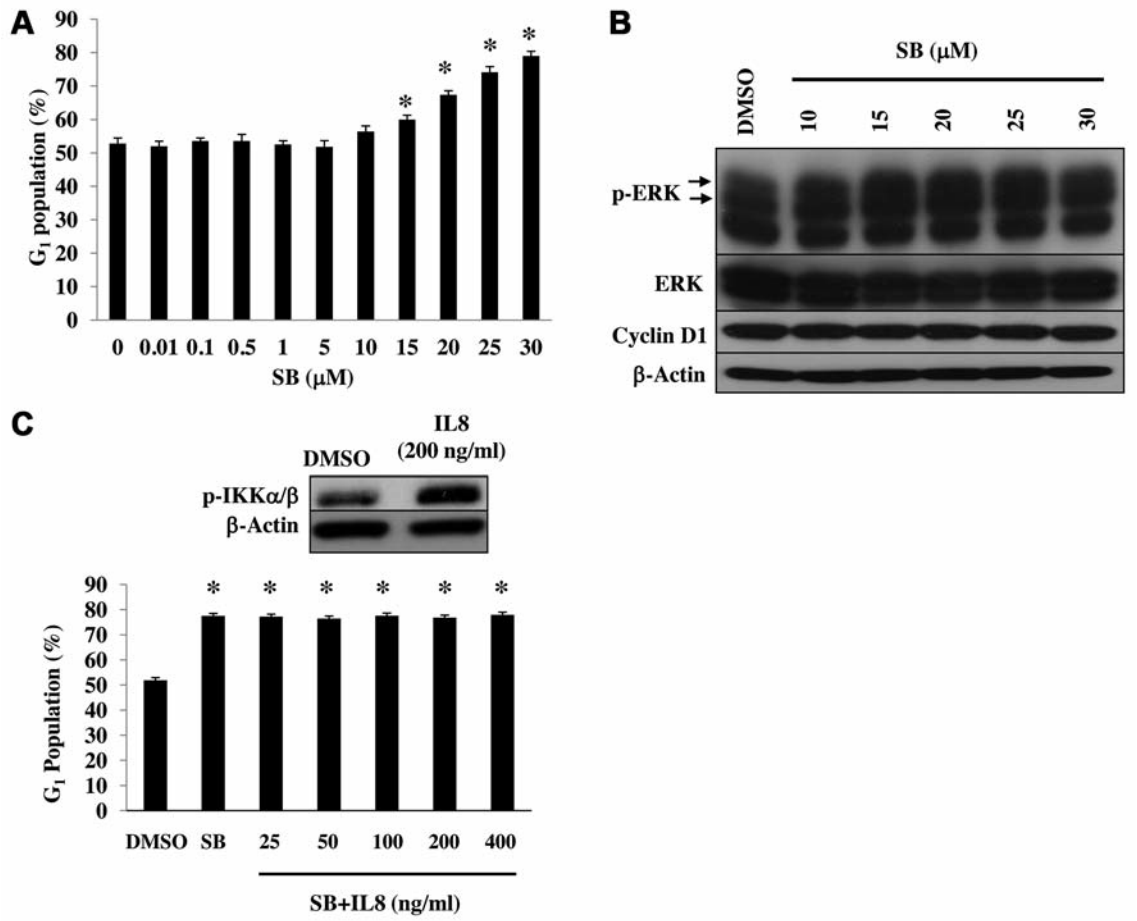

Figure 1. *SB265610-induced G_1 arrest in PC-3 cells. A: Flow cytometry analysis of G_1 population in PC-3 cells treated with dimethyl sulfoxide (DMSO) or different concentrations (0.1-30 μM) of SB265610 (SB) for 24 h. B: Immunobloting of p-ERK, total ERK and cyclin D1 in PC-3 cells treated with SB265610 (10-30 μM) for 24 h. C: Upper panel: immunoblotting of IkappaB kinases (IKK)α/β in PC-3 cells treated with IL8 (200 ng/ml) for 60 min. Lower panel: Flow cytometry analysis of G_1 population in PC-3 cells treated with SB265610 alone or in combination with escalating concentrations of IL8 (25, 50, 100, 200, 400 ng/ml) for 24 h. Asterisk indicates a statistically significant difference at $p<0.05$.*

29 ng of cDNA/well). Melting curve analysis was performed following amplification to validate the presence of a single PCR product and the absence of primer dimers. Data were acquired using S1000 thermal cycler and CFX96™ Real-Time PCR Detection Systems and were analyzed using Bio-Rad CFX manager (all BioRad) where the relative abundance of each gene was normalized against 18S rRNA (in each sample) sense: 5`-GTAACCCGTTGAACCCCATT-3`, antisense: 5`-CCATCCAATCGGTAGTAGCG-3` (10). Data representative of three independent experiments (quadruplicates in each) is presented as the mean±SEM. Differences were considered statistically significant at $p<0.05$ using Student's *t*-test.

Results

Characterization of SB265610-induced G_1 arrest in PC3 cells. Since the IL8 pathway is well-known for promoting G_1 progression (1), it was important to design experiments that could distinguish whether SB265610-induced G_1 arrest was an extension of the pharmacological activity of this inhibitor or occurred through interference with an alternative signaling pathway. To this end, we selected PC-3 prostate carcinoma cells as a model cell line because the consequences of IL8 deprivation in this cell line have previously been characterized (11). Treatment of PC-3 cells with SB265610 at 0.01-5 μM which flank the concentrations selective for CXCR2 receptors (12) did not induce G_1 arrest as assessed by flow cytometry analysis (Figure 1A). However, higher SB265610 concentrations (10, 15, 20, 25 and 30 μM) which lack CXCR2 selectivity induced G_1 arrest (Figure 1A). To confirm that the observed G_1 arrest was not due to interference with IL8 signaling, we analyzed the expression of two IL8 downstream targets, phosphorylated ERK (p-ERK) and cyclin D1 which are known to be positively regulated by IL8 (11). Immunoblot analysis of PC-3 cells treated with the same G_1 arrest-

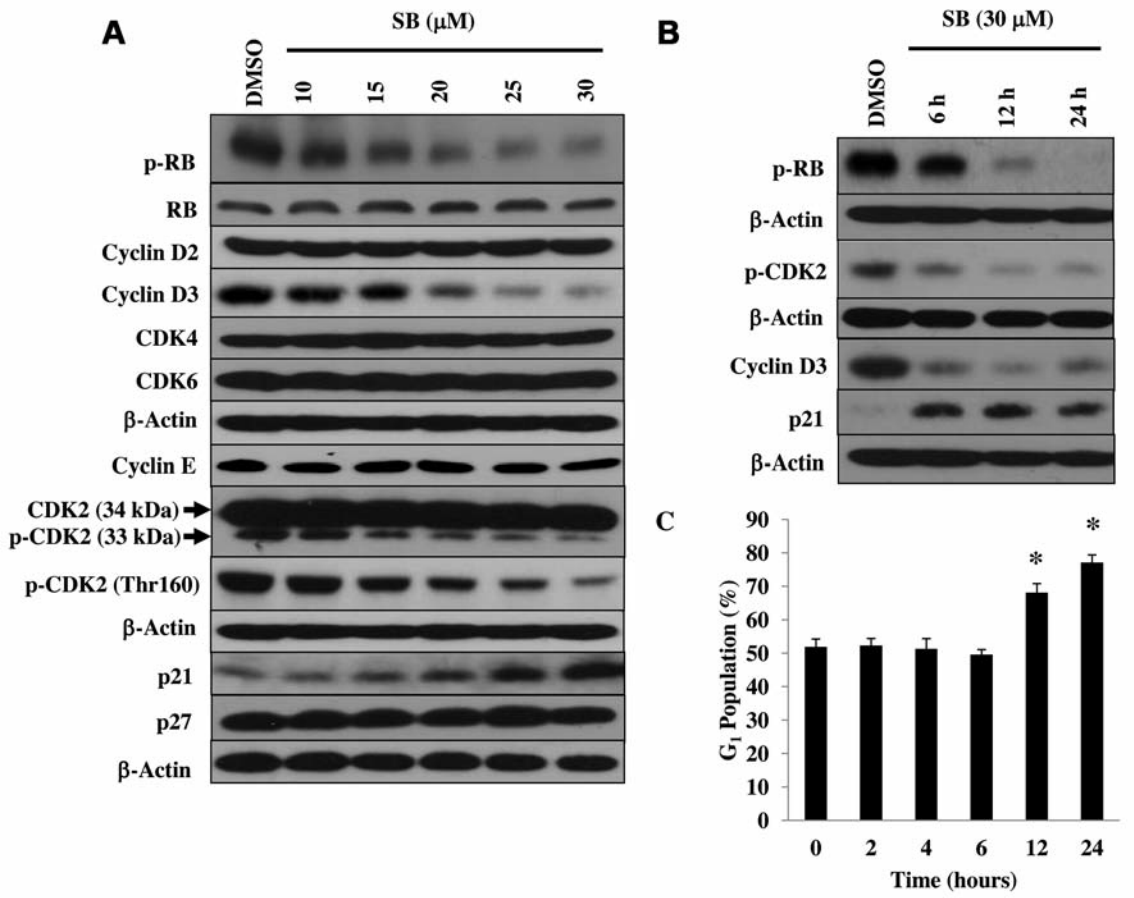

Figure 2. *SB265610-induced G_1 arrest is associated with hypophosphorylation of RB (Ser795) and CDK2 (Thr160), down-regulation of cyclin D3 and induction of p21 in PC-3 cells. A: Immunoblot analysis of different G_1 regulators in PC-3 cells treated with SB265610 (10-30 μM) for 24 h. B: Time-course immunoblot analysis of phospho-RB, p-CDK2, cyclin D3 and p21 in PC-3 cells treated with SB (30 μM) for 6, 12, 24 hours. C: Time-course flow cytometry analysis of G_1 population in PC-3 treated with SB (30 μM) for 6, 12, and 24 h. Asterisk indicates a statistically significant difference at $p<0.05$.*

inducing concentrations of SB265610 revealed that the expression of p-ERK and cyclin D1 remained unchanged (Figure 1B). Taken together, these findings suggested that SB265610-induced G_1 arrest was not mediated through inhibition of IL8 signaling in PC-3 cells.

Furthermore, we investigated whether the exogenously added recombinant human IL8 might affect SB265610-induced G_1 arrest. To this end, we firstly validated the functionality of the exogenously supplemented IL8 in PC-3 cells. Immunoblot analysis showed that IL8 treatment induced a robust increase in IKKα/β phosphorylation (Figure 1C top panel). Next, PC-3 cells were challenged with escalating concentrations of IL8 for 30 min before being co-treated with SB265610 (30 μM) for an additional 24 h, then cells were subjected to flow cytometry analysis. Results revealed the persistence of G_1 arrest even at relatively high IL8 concentrations (up to 400 ng/ml) (Figure 1C).

SB265610 triggered hypophosphorylation of RB and CDK2 (Thr160), down-regulated cyclin D3, and induced p21 expression in PC-3 cells. To identify the mediators of SB265610-induced G_1 arrest in PC-3 cells, the expression of different G_1 regulators was profiled. Immunoblot analysis was carried out for RB and its upstream cyclin-dependent kinases (CDKs) along with their cyclin binding partners. In addition, CDK inhibitors p21 and p27 were also examined. Results showed a dose-dependent hypophosphorylation of RB (Ser795) and suppression of cyclin D3 levels following SB265610 treatment for 24 h (Figure 2A). Although there was no change in the expression level of the 34-kDa CDK2 band, which corresponds to inactive CDK2 (13, 14) (Figure 2A), a dose-dependent down-regulation in the faster migrating 33-kDa CDK2 band was detected, which corresponds to active CDK2 (Thr160-phosphorylated and Tyr15-dephosphorylated) (13, 14) (Figure 2A). This was

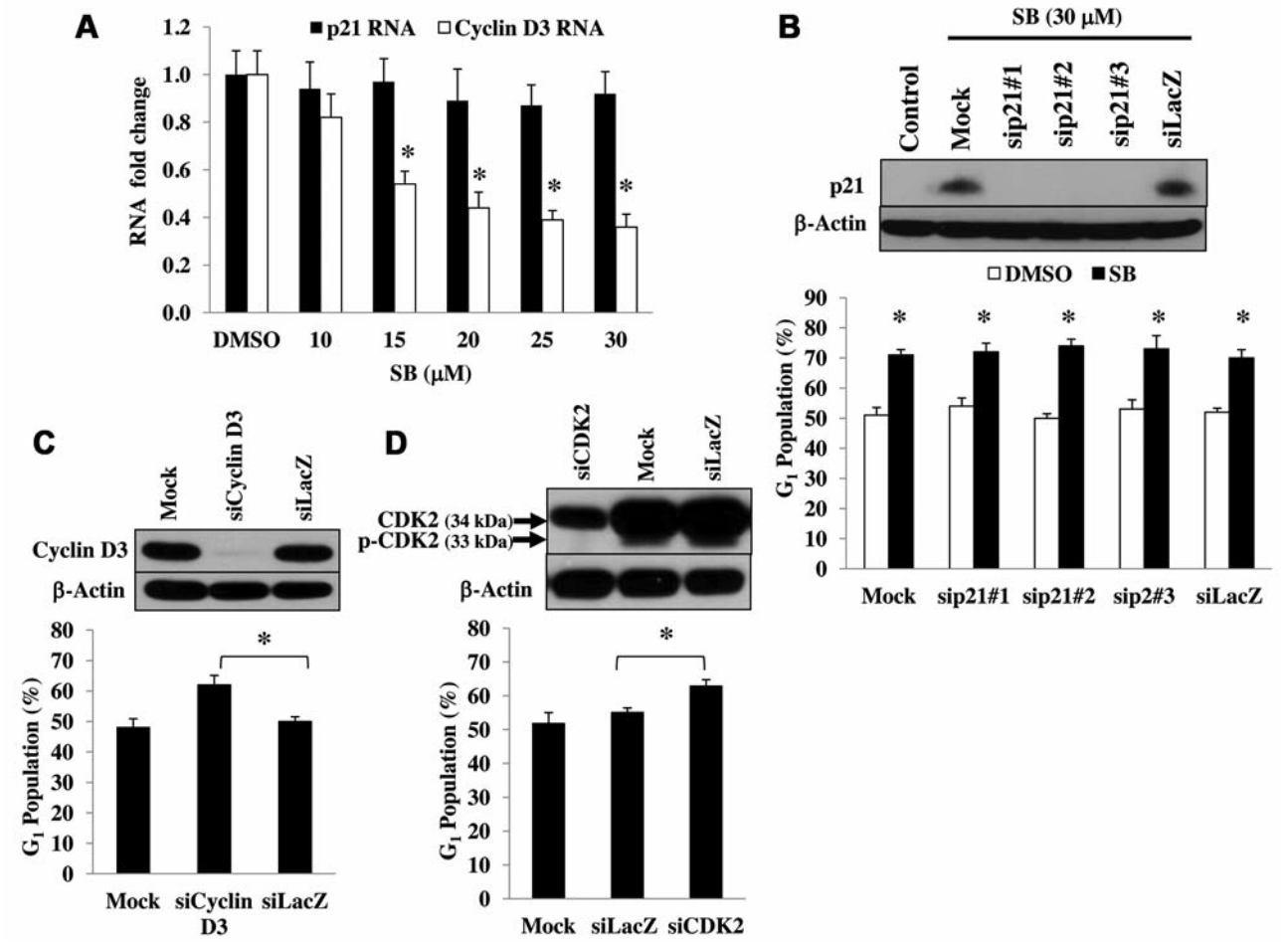

Figure 3. *Down-regulation of cyclin D3 RNA but not that of p21 by SB265610, and the differential contribution of cyclin D3, CDK2 and p21 to SB265610-induced G_1 arrest in PC-3 cells. A: Real-time PCR analysis of cyclin D3 and p21 RNA levels in PC-3 cells following treatment with different concentrations of SB265610 for 24 h. B: Upper panel: Immunoblotting of p21 levels (SB265610-induced for 24 h) in PC-3 cells following siRNA-mediated gene knockdown using three different targeting sequences of p21 siRNA. Lower panel: Flow cytometry analysis of G_1 population in PC-3 cells transfected with LacZ siRNA or with three different targeting sequences of p21 siRNA then treated with SB (30 μM) for 24 h. C: Upper panel: Immunoblot analysis of cyclin D3 levels following siRNA-mediated gene knockdown of cyclin D3 for 48 h in PC-3 cells. Lower panel: Flow cytometry analysis of G_1 population in PC-3 cells transfected with cyclin D3 siRNA for 48 h. D: Upper panel: Immunoblot analysis of CDK2 levels following siRNA-mediated gene knockdown of CDK2 for 48 h in PC-3 cells. Lower panel: Flow cytometry analysis of G_1 population in PC-3 cells transfected with CDK2 siRNA for 48 h. Asterisk indicates a statistically significant difference at $p<0.05$.*

further confirmed by immunoblot analysis of CDK2 (Thr160) phosphorylation, which is essential for CDK2 activity (13). Results showed a concentration-dependent (Thr160) hypophosphorylation of CDK2 by SB265610 treatment (Figure 2A). With regard to the expression level of CDK inhibitors, immunoblotting showed that p21 protein but not p27 protein was up-regulated by SB265610 in a dose-dependent manner (Figure 2A).

Further, the expression changes in phospho(Ser795)-RB, phospho(Thr160)-CDK2, cyclin D3 and p21 were investigated by immunoblotting after different time points of exposure to SB265610 (30 μM). Results showed that the expression levels of phospho(Ser795)-RB and phospho(Thr160)-CDK2 were partially down-regulated after 6 h and were almost completely suppressed after 24 h (Figure 2B). With regards to cyclin D3, the minimum expression was attained after 12 h of treatment, with partial but a very weak recovery after 24 h, which resembled its expression level after 6 h of treatment (Figure 2B). Concerning p21, a strong induction was observed as early as 6 h of treatment which further increased in magnitude, reaching a maximum after 12 h, declining moderately thereafter (Figure 2B). Moreover, to

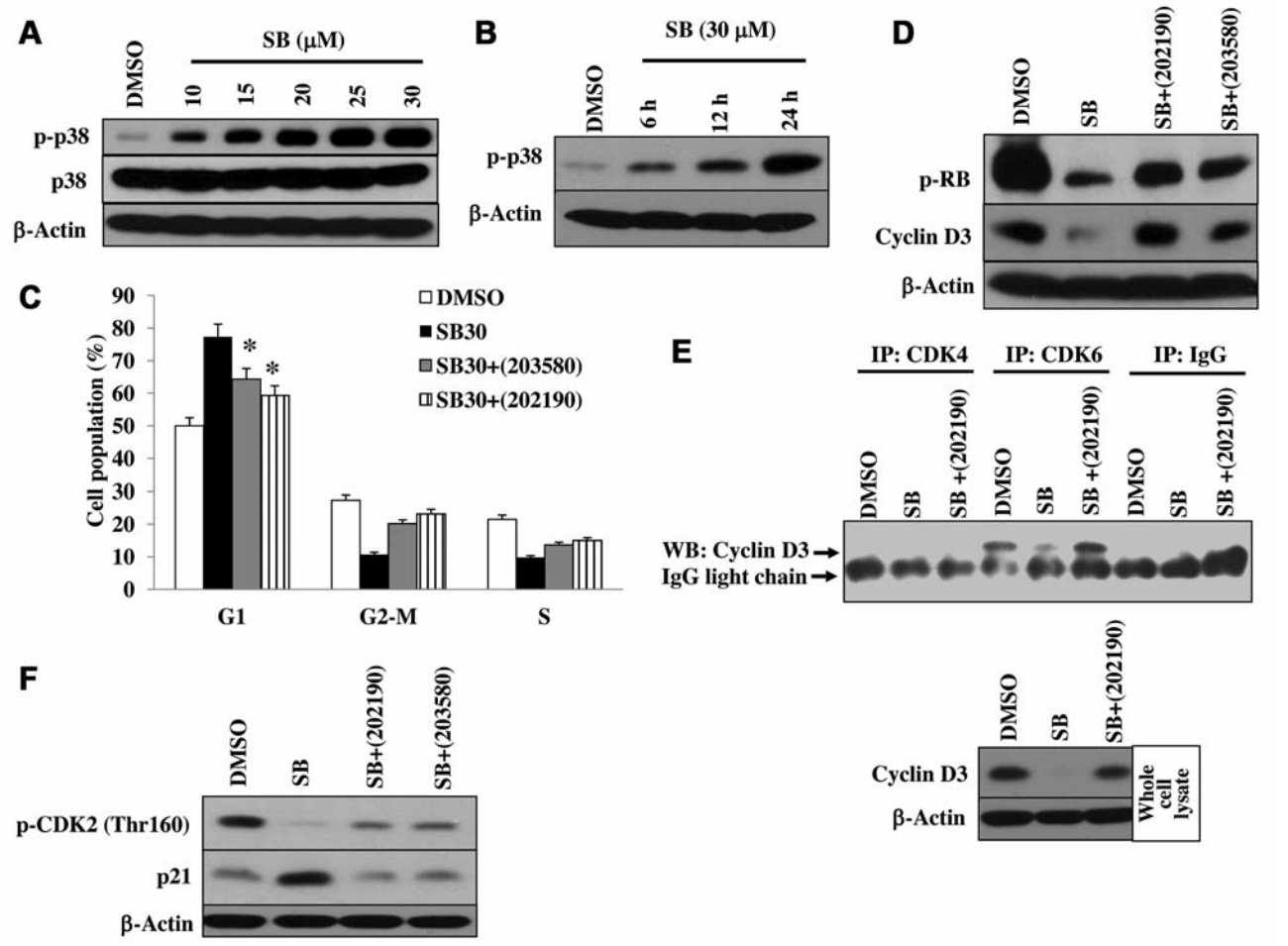

Figure 4. *SB265610 activated p38MAPK which regulated G_1 progression in PC-3 cells. A: Immunobloting of phospho- and total p38MAPK in PC-3 cells treated with SB265610 (10-30 μM) for 24 h. B: Time-course immunoblot analysis of phospho-p38MAPK in PC-3 cells treated with SB (30 μM) for 6, 12, 24 h. C: Flow cytometry analysis of cell cycle populations (G_1, S, G_2-M) in PC-3 cells pretreated with two specific p38MAPK inhibitors, SB202190 (5 μM) or SB203580 (10 μM) for 2 h followed by co-treatment with SB265610 (30 μM) for 24 h. D: Immunoblot analysis of the effect of p38MAPK chemical inhibition on the phosphorylation status of RB and expression level of cyclin D3 in PC-3 cells pre-treated with two specific p38MAPK inhibitors, SB202190 (5 μM) or SB203580 (10 μM) for 2 h then co-treated with SB265610 (30 μM) for 24 h. E: Upper panel: Immunoprecipitation (IP) of CDK4, CDK6 or IgG followed by immunoblotting (WB) of cyclin D3 in PC-3 cells treated with SB265610 (30 μM) for 24 h in the presence or absence of p38MAPK inhibitor SB202190 (5 μM, 2 h pre-treatment). Lower panel: immunoblot analysis of cyclin D3 in whole cell lysate samples of PC-3 cells treated with SB265610 (30 μM) for 24 h in the presence or absence of p38MAPK inhibitor SB202190 (5 μM, 2 h pre-treatment). F: Immunoblot analysis of the effect of p38MAPK chemical inhibition on the phosphorylation status of CDK2 and expression level of p21 in PC-3 cells pretreated with two specific p38MAPK inhibitors, SB202190 (5 μM) or SB203580 (10 μM) for 2 h followed by co-treatment with SB265610 (30 μM) for 24 h. Asterisk indicates a statistically significant difference at $p<0.05$.*

explore the potential correlation of the induction of G_1 arrest by SB265610 (30 μM) treatment with the time-course changes in the expression of G_1 regulators, flow cytometry analysis was performed. Results showed that PC-3 cells were significantly arrested in G_1 after 12 h, with a maximum increase observed after 24 h (Figure 2C). These results indicated that the kinetics of G_1 arrest induced by SB265610 was very closely associated with the observed modulations in the expression of G_1 regulators (Figure 2B).

Differential contribution of G_1 regulators modulated by SB265610 to G_1 arrest in PC-3 cells. Next, we investigated whether the observed expression changes in cyclin D3 and p21 were due to modulation of their gene expression. To this end, real-time PCR was carried-out on PC-3 cells following SB265610 treatment to assess the expression of *CCND3* (cyclin D3) and *CDKN1A* (p21). Results showed that only *CCND3* (cyclin D3) RNA levels were dose-dependently inhibited, while *CDKN1A* (p21) RNA levels remained

unchanged (Figure 3A), suggesting that SB265610 induced *CDKN1A* (p21) expression *via* a post-translational mechanism.

To further gain insights into the relative contribution of p21 to SB265610-induced G_1 arrest in PC-3 cells, RNA interference was performed. Flow cytometry analysis of PC-3 cells transfected with siRNA sequence #1 (sip21#1) interestingly showed that knockdown of *CDKN1A* (p21) expression did not affect SB265610-induced G_1 arrest despite that p21 protein levels were efficiently suppressed (Figure 3B). This finding was further reproduced using two different siRNA sequences (sip21#2 and sip21#3), where SB265610-induced p21 expression was completely suppressed, while G_1 arrest persisted (Figure 3B). Taken together, these results strongly indicated that p21 was dispensable for SB265610-induced G_1 arrest in PC-3 cells.

Given the functional overlap among D-type cyclins (15), we examined the impact of cyclin D3 down-regulation by SB265610 in PC-3 cells. Knockdown of *CCND3* (cyclin D3) expression (Figure 3C, upper panel) resulted in the retardation of G_1 cell-cycle progression of PC-3 cells as assessed by flow cytometry analysis (Figure 3C, lower panel), indicating that cyclin D3 plays a non-redundant role in the G_1 transit of PC-3 cells. This finding emphasized the importance of cyclin D3 down-regulation as a mediator of SB265610-induced G_1 arrest.

Moreover, we investigated whether the modulation of CDK2 phosphorylation status by SB265610 treatment might have a functional consequence on cell-cycle progression given that CDK2 activity is dispensable in some cancer cells (16). To mimic this situation, a *CDK2* siRNA approach was followed in PC-3 cells. Immunoblotting of PC-3 cell lysates harvested 48 h after *CDK2* siRNA transfection showed that both the 34 and 33 KDa bands of CDK2 were efficiently down-regulated (Figure 3D, upper panel). Furthermore, flow cytometry analysis showed that *CDK2* siRNA-transfected PC-3 cells were arrested in G_1 (Figure 3D, lower panel), indicating that CDK2 is required for G_1 transition in PC-3 cells, reflecting the potential significance of the suppression of CDK2 (Thr160) phosphorylation by SB265610 treatment.

Activation of p38MAPK by SB265610 regulated cyclin D3 expression and significantly contributed to induction of G_1 arrest in PC-3 cells. Next, we investigated the upstream signaling pathways which might mediate the observed expression changes in the G_1 regulators and cell-cycle arrest by SB265610 treatment of PC-3 cells. Cell-cycle progression is well-known to be regulated by members of the mitogen-activated protein kinase (MAPK) family (17) and by the protein kinase B (PKB/AKT) pathway (18). Therefore, we investigated whether any of these signaling pathways could mediate SB265610-induced G_1 arrest. Treatment of PC-3 cells with SB265610 did not inhibit the phosphorylation of ERK (Figure 1B), c-Jun N-terminal kinase (JNK) nor PKB/AKT (data not shown). Interestingly, SB265610-treated PC-3 cells showed dose-dependent increments in the phosphorylation of the p38MAPK (Figure 4A). Furthermore, time-course immunoblotting revealed that SB265610 (30 μM) induced a progressive and sustained activation of p38MAPK phosphorylation which was detected after 6 hours and attained a maximum after 24 hours of treatment (Figure 4B). These results were closely associated with SB265610-induced expression changes in G_1 regulators (Figure 2B), as well as G_1 arrest induction (Figure 2C).

To establish a cause-effect relationship between SB265610-induced p38MAPK activation and G_1 arrest, the impact of pharmacological interference with p38MAPK signaling was investigated using two specific small-molecule inhibitors of p38MAPK, SB202190 and SB203580. PC-3 cells were pretreated with either of these two inhibitors prior to SB265610 application, and samples were harvested after 24 h for the assessment of cell-cycle profile and immunoblotting of the (Ser795)-phosphorylated RB and cyclin D3 levels. Flow cytometry analysis showed that SB202190 and SB203580 brought about 47% and 65% reductions, respectively, in the magnitude of G_1 arrest induced by SB265610 treatment (Figure 4C). These findings indicated that p38MAPK signaling was a major contributor to SB26510-induced G_1 arrest. Moreover, immunoblot analysis revealed a marked but partial recovery of the phosphorylated RB levels and a complete restoration of cyclin D3 expression (Figure 3D), suggesting that SB265610-induced RB (Ser795)-hypophosphorylation was not exclusively dependent on p38MAPK-mediated cyclin D3 down-regulation.

Given that cyclin D3 can bind to CDK4 or CDK6 (14), we characterized the CDK binding partner of cyclin D3 in PC-3 cells. Immunoprecipitation showed that in untreated cells, cyclin D3 was bound to CDK6 but not CDK4 (Figure 4E, upper panel). Treatment with SB265610 abrogated cyclin D3-CDK6 interaction due to the suppression of cyclin D3 expression (Figure 4E, lower panel). Of note, pre-treatment with p38MAPK inhibitor normalized cyclin D3 levels (Figure 4E, lower panel) and restored its binding to CDK6 (Figure 4E, upper panel). This finding indicated that down-regulation of cyclin D3 by SB265610 treatment mainly affected cyclin D3–CDK6 complex in PC-3 cells.

It was interesting to determine whether CDK2 (Thr160)-phosphorylation might be affected by pharmacological interference with p38MAPK signaling. In PC-3 cells, immunoblotting showed that p38MAPK inhibitors weakly restored SB265610-triggerred CDK2 (Thr160) hypo-phosphorylation, even though p21 expression was completely abrogated (Figure 4F). These findings uncoupled the p38MAPK-dependent p21 induction from CDK2 (Thr160) hypophosphorylation, an event that appeared to be largely p38MAPK-independent.

Discussion

In the present study, we endeavored to characterize the mechanisms underlying induction of G_1 arrest by SB265610, a highly selective CXCR2 antagonist. Results described herein provided evidence for the involvement of cyclin D3 and CDK2 in G_1 arrest induction by SB265610. However, p21 was confirmed to be dispensable for SB265610-induced G_1 arrest, a situation which is not uncommon (19). These findings cannot be explained on the basis of inhibition of IL8 receptors. Furthermore, several pieces of evidence also suggested the independence of SB265610-induced G_1 arrest of IL8 signaling including: the CXCR2-non selective concentration range (12) over which G_1 arrest was induced, the lack of expression changes of IL8 downstream targets, cyclin D1 and ERK (11), and p38MAPK activation. Therefore, these findings can qualify as novel mechanisms of SB265610 action, and may explain, at least in part, why G_1 arrest induced by SB265610 was not overridden by the exogenously supplemented IL8.

Moreover, we demonstrated that CDK6, but not CDK4, was the binding partner of cyclin D3 in PC-3 cells. Since knockdown of cyclin D3 *per se* was sufficient to induce G_1 arrest, this implied that other D-type cyclins, cyclin D1 and cyclin D2 could not compensate for cyclin D3 deficiency, which in turn highlighted the potential role of cyclin D3-CDK6 complex in driving the G_1 transition in PC-3 cells. Therefore, down-regulation of cyclin D3 is an important molecular target for SB265610 since it can evade redundancy among D-type cyclins (15), and may explain, at least in part, the observed Ser795 hypophosphorylation of RB.

Results of the current study and our previous findings (4) have demonstrated the sustained activation of p38MAPK by two structurally-related CXCR2 antagonists of the diarylurea class, namely SB265610 and SB225002, despite that the consequences of such activation were different. Of note, the role of p38MAPK in regulating the G_1 cell-cycle progression is well documented (20). Moreover, p38MAPK activation by SB265610 differentially affected the G_1 regulators in PC-3 cells, where the expression changes of cyclin D3 and p21 were p38MAPK-dependent, while that of (Thr160) phosphorylation of CDK2 was largely p38MAPK-independent. The latter finding is contradictory to a previous report (21) and most likely is due to the differences in the nature and origin of the cell lines used (rodent versus human cell lines). This (Thr160) hypophosphorylation of CDK2 by SB265610 treatment may explain, at least in part, the p38MAPK-independent RB (Ser795) hypophosphorylation in PC-3 cells. Of note, the detailed mechanisms underlying the down-regulation of *CCND3* (cyclin D3) and CDK2 (Thr160) hypo-phosphorylation in PC-3 cells following SB265610 treatment are yet to be uncovered.

In summary, findings of the present study introduced novel mechanisms underlying the antitumor activity of SB265610 which could be of therapeutic value in overriding cancer cell proliferation in IL8-rich tumor microenvironments.

Acknowledgements

This work was supported by the World Class Institute (WCI 2009-002) program, global R&D center (GRDC) program, Bio & Medical Technology Development Program (NRF-2014M3A9B5073938) of the NRF, and KRIBB Research Initiative Program funded by the Ministry of Science, ICT and Future Planning (MSIP), Republic of Korea.

Conflicts of Interest

The Authors declare no conflict of interest with regard to this study.

References

1 Waugh DJ and Wilson C: The interleukin-8 pathway in cancer. Clin Cancer Res *14*: 6735-6741, 2008.

2 Bizzarri C, Beccari AR, Bertini R, Cavicchia MR, Giorgini S and Allegretti M: ELR+ CXC chemokines and their receptors (CXC chemokine receptor 1 and CXC chemokine receptor 2) as new therapeutic targets. Pharmacol Ther *112*: 139-149, 2006.

3 Stadtmann A and Zarbock A: CXCR2: From bench to bedside. Front Immunol *3*: 263:1-12, 2012.

4 Goda AE, Koyama M, Sowa Y, Elokely KM, Yoshida T, Kim BY and Sakai T: Molecular mechanisms of the antitumor activity of SB225002: a novel microtubule inhibitor. Biochem Pharmacol *85*: 1741-1752, 2013.

5 Goda AE, Yoshida T, Horinaka M, Yasuda T, Shiraishi T, Wakada M and Sakai T: Mechanisms of enhancement of TRAIL tumoricidal activity against human cancer cells of different origin by dipyridamole. Oncogene *27*: 3435-3445, 2008.

6 Aliouat-Denis CM, Dendouga N, Van den Wyngaert I, Goehlmann H, Steller U, van de Weyer I, Van Slycken N, Andries L, Kass S, Luyten W, Janicot M and Vialard JE: p53-independent regulation of $p21^{Waf1/Cip1}$ expression and senescence by Chk2. Mol Cancer Res *3*: 627-634, 2005.

7 Tan HH and Porter AG: p21(WAF1) negatively regulates DNMT1 expression in mammalian cells. Biochem Biophys Res Commun *382*: 171-176, 2009.

8 Bryant P, Zheng Q and Pumiglia K: Focal adhesion kinase controls cellular levels of p27/Kip1 and p21/Cip1 through Skp2-dependent and -independent mechanisms. Mol Cell Biol *26*: 4201-4213, 2006.

9 Pallet N, Thervet E, Le Corre D, Knebelmann B, Nusbaum P, Tomkiewicz C, Meria P, Flinois JP,Beaune P, Legendre C and Anglicheau D: Rapamycin inhibits human renal epithelial cell proliferation: effect on cyclin D3 mRNA expression and stability. Kidney Int *67*: 2422-2433, 2005.

10 Schmittgen TD and Zakrajsek BA: Effect of experimental treatment on housekeeping gene expression: validation by real-time, quantitative RT-PCR. J Biochem Biophys Methods *46*: 69-81, 2000.

11 Singh RK and Lokeshwar BL: Depletion of intrinsic expression of Interleukin-8 in prostate cancer cells causes cell cycle arrest, spontaneous apoptosis and increases the efficacy of chemotherapeutic drugs. Mol Cancer *8*: 57-71, 2009.
12 White JR, Lee JM, Young PR, Hertzberg RP, Jurewicz AJ, Chaikin MA, Widdowson K, Foley JJ, Martin LD, Griswold DE and Sarau HM: Identification of a potent, selective non-peptide CXCR2 antagonist that inhibits interleukin-8-induced neutrophil migration. J Biol Chem *273*: 10095-10098, 1998.
13 Gu Y, Rosenblatt J and Morgan DO: Cell-cycle regulation of CDK2 activity by phosphorylation of Thr160 and Tyr15. EMBO J *11*: 3995-4005, 1992.
14 Morgan DO: Cyclin-dependent kinases: engines, clocks, and microprocessors. Annu Rev Cell Dev Biol 13: 261-291, 1997.
15 Sherr CJ and Roberts JM: Living with or without cyclins and cyclin-dependent kinases. Genes Dev *18*: 2699-2711, 2004.
16 Grim JE and Clurman BE: Cycling without CDK2? Trends Cell Biol *13*: 396-399, 2003.
17 MacCorkle RA and Tan TH: Mitogen-activated protein kinases in cell-cycle control. Cell Biochem Biophys *43*: 451-461, 2005.
18 Chang F, Lee JT, Navolanic PM, Steelman LS, Shelton JG, Blalock WL, Franklin RA and McCubrey JA: Involvement of PI3K/AKT pathway in cell cycle progression, apoptosis, and neoplastic transformation: a target for cancer chemotherapy. Leukemia *17*: 590-603, 2003.
19 Chopin V, Toillon RA, Jouy N and Le Bourhis X: P21(WAF1/CIP1) is dispensable for G_1 arrest, but indispensable for apoptosis induced by sodium butyrate in MCF-7 breast cancer cells. Oncogene *23*: 21-29, 2004.
20. Thornton TM and Rincon M: Non-classical p38 MAP kinase functions: cell cycle checkpoints and survival. Int J Biol Sci *5*: 44-51, 2009.
21 Corrèze C, Blondeau JP and Pomérance M: p38 Mitogen-activated protein kinase contributes to cell-cycle regulation by cAMP in FRTL-5 thyroid cells. Eur J Endocrinol *153*: 123-133, 2005.

Received February 15, 2015
Revised February 26, 2015
Accepted March 2, 2015